Generation and Load Balance Using Linear Quadratic Gaussian Control

Abdullah Al-Digs and Yu Christine Chen
Department of Electrical and Computer Engineering
The University of British Columbia
Vancouver, BC V6T 1Z4
Email: {aldigs, chen}@ece.ubc.ca

***Abstract*—The state-space model-based control design for a two-area interconnected AC electric power system using the linear quadratic gaussian (LQG) controller is realized in this paper. In industry, the classical integer-order proportional-integral (PI) and proportional-integral-derivative (PID) controllers have been broadly adopted for automatic generation control (AGC). The conventional PI and PID controllers leverage area control error (ACE) measurements to eliminate steady-state errors in frequency and tie-line interchange active-power flow. This paper presents a comparison amongst the dynamic response of the conventional PI controller and observer-based servo controllers designed using pole placement as well as LQG techniques. The overarching goal of this work is to improve the dynamic response of AGC systems through an optimal control method, namely, LQG. This paper investigates AGC systems for interconnected power systems and shows that LQG controllers perform better than both the classical PI controller as well as the observer-based one designed using pole placement.**

I. Introduction

This paper presents a design for an Automatic Generation Control (AGC) system using linear quadratic gaussian (LQG) controller design in an AC power system assumed to operate in sinusoidal steady state, i.e., voltages and currents are represented as phasors. In particular, we consider the setting of the bulk AC power system, which is divided into multiple control areas, with synchronous generators supplying constant-power loads through a linear time-invariant electrical network.

To ensure reliable and secure power system operation and control, generation and load balance is necessary to maintain the nominal operating frequency and scheduled tie-line interchange power flow [1]. This is achieved by the AGC system in an interconnected power system. As the load demand varies randomly, the system frequency and tie-line power interchange also vary [2]. The AGC system aims to maintain system frequency at the nominal value, maintain generation of individual units at the most economic value, and keep the correct value of tie-line power flow between different control areas of the power system. The AGC system responds to load changes by adjusting the active-power generation in each control area correspondingly so that frequency and tie-line deviations are suppressed. Additionally, the controller preserves the independence of all control areas by allowing each area to absorb its own load fluctuations. In addition to step load disturbances, the AGC system must also contend with small random disturbances and measurement noise.

Numerous approaches have been applied to tackle the problem of AGC design. The major challenge in this task is due to the nonlinear nature of the power system. Moreover, in general, the system conditions and operating point vary continuously during the daily cycle [3]. Some relevant prior art includes: integer-order PI control that have limitations such as long settling time and large overshoots [4], fuzzy logic control that only replaces the ACE calculation and is usually combined with the existing PI controllers [5], genetic algorithm-based control [6], and active disturbance rejection control [7]. The method proposed in this paper is unique in that it guarantees robustness and optimal tracking trajectory response using linear quadratic regulator (LQR) regardless of disturbances and initial conditions. Given that pertinent system information (such as load changes, topological changes, and system parameters) are, in general, not readily available, the controller incorporates an optimal estimator, namely the Kalman filter, which accounts for disturbances and measurement noise. Thus, the proposed controller is less sensitive to exogenous disturbances and plant perturbations.

Traditionally, the AGC system's main goals are to maintain system frequency, scheduled tie-line flow, and economic operation of fuel-based generators. However, with the penetration of renewable resources and given the prevalent competitive electricity environment, the various functions of AGC are potentially useful in a variety of settings to ensure that electricity markets can be operated in a fair and efficient manner. For example, maintaining tie-line flow can be more broadly applied as individual line-flow control, which may be used to reduce congestion rents. Steering clear of specific power-system applications, this paper illustrates ideas by focusing on a two-area power system and showing the dynamic response of three different controllers to rapid step load changes and system frequency variations. The controllers examined in this work are (i) a conventional PI controller using the transfer-function approach, which is tuned through trial and error, (ii) an observer-based controller consisting of a state-feedback controller combined with a full-dimensional observer, which is tuned using the pole placement technique, leading to more predictive behaviour because pole locations can be chosen precisely, and (iii) an LQG controller consisting of an LQR controller combined with a Kalman filter, which is tuned by selecting LQR performance index weighting factors.

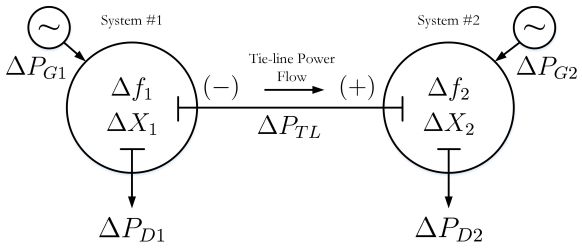

Fig. 1: Two-area interconnected AC power system.

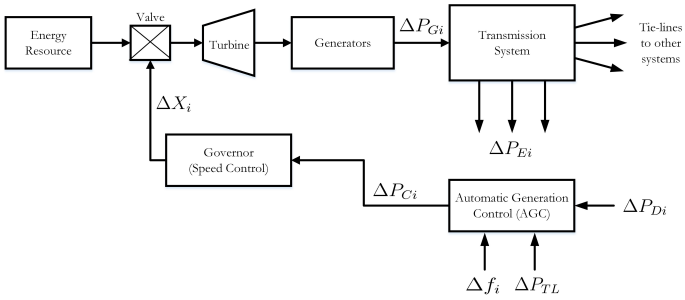

Fig. 2: Individual control area subsystem.

II. System Description and Analysis

Consider the two-area interconnected power system shown in Fig. 1 and assume that it is in pseudo steady state with voltages and currents represented as phasors; system dynamics arise from generators and loads. The network consists of two independent subsystems referred to as control areas, each of which utilizes its own AGC system. We note that the subsystems are independent in the sense that each control area is responsible for absorbing its own load changes. Each control area consists of the subsystem shown in Fig. 2, where the generators supply the loads through transmission lines. Balancing generation and load eliminates frequency deviations only. To ensure that tie-line interchange deviations from scheduled transactions are eliminated as well, each area must absorb its own load variations. The control areas are connected via interchange transmission lines where power can flow from one area to another. This is usually done for economic and reliable operation in case of contingencies [8].

With respect to Fig. 1, denote the changes in frequency, valve position, power generation, active-power tie-line flow, speed changer setting, and power demand, by Δf, ΔX, ΔP_G, ΔP_{TL}, ΔP_C, and ΔP_D, respectively. The overall control objective of AGC system is to eliminate steady-state error in Δf and ΔP_{TL}, which are the monitored outputs. Load changes in the system ΔP_D behave as step disturbance. The control input of the AGC system in each area is ΔP_C, which feeds into the governor, subsequently changes ΔX to allow more or less primary fuel source through the turbine, and ultimately adjusts power generation ΔP_G. The assumptions made in multi-area power system control are that (i) the overall governing characteristics of the operating units in any area can be represented by linear curves of frequency versus generation, (ii) governors in all areas start acting simultaneously to changes in their respective areas, and (iii) secondary control devices act after the initial governor response is complete [9].

A. Modelling

The interconnected power system in Fig. 1 is represented using a small-signal model linearized around a steady-state operating point. Referring to Fig. 2, the electrical load, generator, governor (speed controller), turbine (prime mover), and tie-line blocks in control area i (where $i = 1$ or 2) are modelled as follows [10]. The aggregate electrical load is modelled using

$$\Delta P_{Ei} = \Delta P_{Di} \pm \Delta P_{TL} + \frac{1}{K_{psi}} \Delta f_i. \tag{1}$$

TABLE I: Parameters values used in two-area system in Fig. 1.

Control Area 1	Control Area 2
$K_{ps1} = 120$	$K_{ps2} = 100$
$T_{ps1} = 20$ s	$T_{ps2} = 22$ s
$T_{sg1} = 0.2$ s	$T_{sg2} = 0.3$ s
$R_1 = 2.5$	$R_2 = 3$
$T_{t1} = 0.4$ s	$T_{t2} = 0.5$ s
$T_{12} = 0.0127$	$T_{12} = 0.0127$

The electrical generator is modelled using

$$\Delta \dot{f}_i = \frac{K_{psi}}{T_{psi}} \Delta P_{Gi} - \frac{1}{T_{psi}} \Delta f_i - \frac{K_{psi}}{T_{psi}} \Delta P_{Di} \pm \frac{K_{psi}}{T_{psi}} \Delta P_{TLi}, \tag{2}$$

with the combined governor/turbine modelled as

$$\Delta \dot{X}_i = \frac{1}{T_{sgi}} \Delta P_{Ci} - \frac{1}{T_{sgi}} \Delta X_i - \frac{1}{R_i T_{sgi}} \Delta f_i, \tag{3}$$

$$\Delta \dot{P}_{Gi} = \frac{1}{T_{ti}} \Delta X_i - \frac{1}{T_{ti}} \Delta P_{Gi}. \tag{4}$$

Finally, dynamics in the tie-line flow are modelled using

$$\Delta \dot{P}_{TL} = 2\pi T_{12} (\Delta f_1 - \Delta f_2). \tag{5}$$

In (1)–(5), K_{psi} denotes the power system gain constant for area i; T_{psi}, T_{sgi}, and T_{ti} denote the power system, governor, and turbine time constants, respectively; for the generator in area i, R denotes the governor droop (speed regulation) constant; and T_{12} denotes the maximum tie-line active-power flow. For the system shown in Fig. 1, the values for the aforementioned parameters are reported in Table I. The values are chosen from a range of typical values for these constants [9].

B. State-space Model

Define state, input, disturbance, and output vectors as

$$x = \begin{bmatrix} \Delta f_1 & \Delta f_2 & \Delta X_1 & \Delta X_2 & \Delta P_{G1} & \Delta P_{G2} & \Delta P_{TL} \end{bmatrix}^{\mathrm{T}},$$
$$u = \begin{bmatrix} \Delta P_{C1} & \Delta P_{C2} \end{bmatrix}^{\mathrm{T}}, \quad w = \begin{bmatrix} \Delta P_{D1} & \Delta P_{D2} \end{bmatrix}^{\mathrm{T}},$$
$$y = \begin{bmatrix} \Delta f_1 & \Delta P_{TL} \end{bmatrix}^{\mathrm{T}},$$

respectively. With the component models described in (1)–(5), the system state-space model for the power system with two interconnected control areas depicted in Fig. 1 can be formulated using the following state and output equations:

$$\begin{cases} \dot{x} = Ax + Bu + B_w w, \\ y = Cx, \end{cases} \tag{6}$$

where matrices A, B, B_w, and C are defined in (7)–(8).

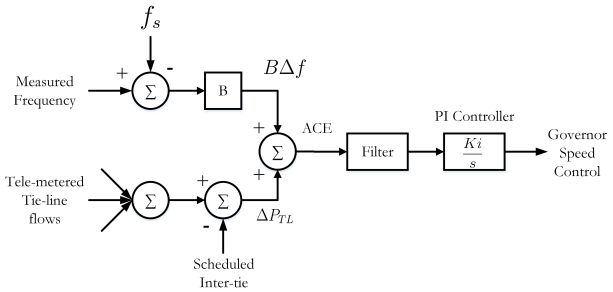

Fig. 3: Block diagram of conventional PI controller using ACE.

C. System Stability, Controllability, and Observability

This section analyzes the system to be controlled in Fig. 1. The analysis is achieved by assessing the stability, controllability, and observability of the overall linearized state-space system model described in (6). These system properties are analyzed separately below.

1) Stability: The stability of the linearized system is assessed using the eigenvalue criterion. The continuous-time (CT) system model in (6) is found to be asymptotically stable with eigenvalues -6.27, $-0.53 \pm \text{j}2.19$, -0.38, $-0.45 \pm \text{j}1.55$, and -4.33. However, some eigenvalues are located near the imaginary axis, which indicates that the system responds slowly to disturbances.

2) Controllability: Designing a successful state feedback control law requires that the system be fully controllable. According to the pole-placement theorem, if (A, B) is controllable, the eigenvalues of the closed-loop system $(A-BK)$ where K is the state-feedback gain, can be placed arbitrarily, provided they are symmetric with respect to the real-axis. The controllability condition requires that the controllability matrix be of full row rank. By checking this condition for the system in (6), we find that the controllability matrix has full rank of 7 and so the system is, indeed, controllable.

3) Observability: Constructing a suitable state-estimator requires that the system be fully observable. When (A, C) is observable, the eigenvalues of $(A - LC)$ where L is the observer gain, can be placed arbitrarily, thus allowing the estimation error to converge to zero asymptotically. Analogous to controllability, the observability condition requires the observability matrix be of full column rank. By checking this condition for the system in (6), we find that the observability matrix has full rank of 7 and so the system is observable.

III. Control Design

This section describes the design aspects of a classical PI controller and observer-based servo controllers using both pole placement and LQG techniques. The PI controller is tuned mainly using trial and error, whereas the observer-based controllers are tuned by placing the pole locations or tuning the LQR performance index weighting factors to minimize the cost function for a suitable feedback control law.

A. PI Controller

The PI controller design is based on classical transfer function control. The PI controller gain is tuned using trial and error. This constant gain is insufficient for the purpose of AGC since the system conditions vary continuously and the operating point changes rapidly. In addition to the unsatisfactory dynamic response trajectory, the response time of the PI controller is very slow. The widely used PI controller in AGC depends on the area control error (ACE) measurement. The ACE is a measure of generation and load imbalance in a power system and is formulated using two indicators, frequency and tie-line deviations, as follows:

$$ACE = \beta \Delta f + \Delta P_{TL}, \tag{9}$$

where Δf represents the difference between the actual and desired system frequency, β represents the control area frequency bias setting, and ΔP_{TL} represents the difference between the actual and desired tie-line interchange. The ACE measurement is then fed to the PI controller, which sends the control input signal to the governor, thereby changing the generation output. The conventional AGC system is illustrated in Fig. 3.

B. Observer-based Servo Controller

The observer-based servo controller is designed using two techniques, namely pole placement and LQG. Both techniques share a common structure consisting of the combination of an observer (state estimator) and a state feedback control law. The state feedback control law is used to both stabilize the closed-loop system poles and enhance the dynamic performance of the controller. This is achieved by the state feedback gain K. The observer is used to estimate the unmeasurable state variables as they are required to design an effective state feedback control law. Denote the state-estimates by $\hat{x}$, which is the output of the observer. While the observer-based controller can regulate the output at a fixed reference point, it would not

$$A = \begin{bmatrix} \frac{-1}{T_{ps1}} & 0 & 0 & 0 & \frac{K_{ps1}}{T_{ps1}} & 0 & \frac{-K_{ps1}}{T_{ps1}} \\ 0 & \frac{-1}{T_{ps2}} & 0 & 0 & 0 & \frac{K_{ps2}}{T_{ps2}} & \frac{K_{ps2}}{T_{ps2}} \\ \frac{-1}{R_1 T_{sg1}} & 0 & \frac{-1}{T_{sg1}} & 0 & 0 & 0 & 0 \\ 0 & \frac{-1}{R_2 T_{sg2}} & 0 & \frac{-1}{T_{sg2}} & 0 & 0 & 0 \\ 0 & 0 & \frac{1}{T_{t1}} & 0 & \frac{-1}{T_{t1}} & 0 & 0 \\ 0 & 0 & 0 & \frac{1}{T_{t2}} & 0 & \frac{-1}{T_{t2}} & 0 \\ 2\pi T_{12} & -2\pi T_{12} & 0 & 0 & 0 & 0 & 0 \end{bmatrix}, \quad B = \begin{bmatrix} 0 & 0 \\ 0 & 0 \\ \frac{1}{T_{sg1}} & 0 \\ 0 & \frac{1}{T_{sg2}} \\ 0 & 0 \\ 0 & 0 \\ 0 & 0 \end{bmatrix}, \quad B_w = \begin{bmatrix} \frac{-K_{ps1}}{T_{ps1}} & 0 \\ 0 & \frac{-K_{ps2}}{T_{ps2}} \\ 0 & 0 \\ 0 & 0 \\ 0 & 0 \\ 0 & 0 \\ 0 & 0 \end{bmatrix} \tag{7}$$

$$C = \begin{bmatrix} 1 & 0 & 0 & 0 & 0 & 0 & 0 \\ 0 & 0 & 0 & 0 & 0 & 0 & 1 \end{bmatrix} \tag{8}$$

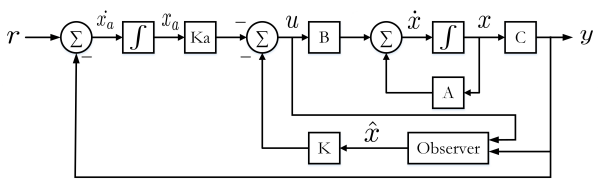

Fig. 4: Block diagram of an observer-based controller.

be able to track a time-varying reference signal. Therefore, the servo (tracking) controller designed utilizes an integrator to eliminate steady-state error where the output follows the reference signal denoted by r very closely. Minimizing steady-state error requires additional states denoted by x_a and an output feedback loop gain K_a. The general structure of the observer-based servo controller is shown as a block diagram in Fig. 4.

1) Pole Placement: Similar to PI control, the pole placement technique requires trial and error. However, it offers more intuition in a general sense towards the effect of the pole locations. The pole placement technique is advantageous due to the existence of general rules of thumb that can be followed. The poles are placed at suitable locations according to the trade-off between convergence time, control input magnitude (saturation), and overshoot. The pole placement technique offers more robustness against step load disturbances and utilizes a full-dimensional observer for estimating the state variables in real time. The estimator poles are placed 5 to 10 times further away from the imaginary axis to allow the state estimates to converge very quickly.

2) Linear Quadratic Gaussian: LQG control is the combination of linear quadratic regulator (LQR) state feedback and Kalman filter state estimator. The LQG controller is optimal in the sense that the LQR state feedback control law requires minimal control signal deviations and the Kalman filter accounts for random disturbances and measurement noise, with which the power system of interest naturally contends. As the system load levels fluctuate and the tie-line interchange varies, the state-feedback and observer gains will automatically provide the optimal trajectory so that the output is either regulated at or tracks the new operating point set by the reference signal. This is achieved, since the solution to the LQR cost function is independent of the initial conditions and system parameters.

The LQG controller is designed for the discretized CT system model in (6). The resulting discrete-time (DT) system is obtained through zero-order-hold (ZOH) discretization method using a sampling time of 17 ms. The sampling time is chosen to be small in order to retain most of the information while also preserving the controllability and observability properties of the resulting DT system. This sampling time is realistic and well within the capability of current measurement technology, e.g., PMUs provide 60 measurement samples per second [11].

The LQR state feedback control law and Kalman filter observer are designed separately and combined afterwards. A DT infinite-horizon LQR control law is designed by specifying the weighting factors of a non-standard LQR cost function. The cost function incorporates the augmented DT system as to add a closed-loop integrator for tracking step inputs and disturbances. As for the observer, a steady-state Kalman filter gain is obtained by incorporating random white-Gaussian disturbances and measurement noise in the system. The load changes are biased step changes, which are decomposed into deterministic (biased) and stochastic (unbiased) components. The deterministic component represents large step disturbances and changes in large loads such as factories, while the stochastic component represents the minor household electrical load variations throughout the day. By incorporating a model for noise, the steady-state error is more realistic and never converges to zero as the loads continuously change in the electrical system. However, the steady-state error is minimized by the LQG controller.

TABLE II: State variables and estimates initial conditions.

State Variable	State Variable Estimates
$\Delta f_1 = 0.05$	$\Delta \hat{f}_1 = 0.02$
$\Delta f_2 = 0.05$	$\Delta \hat{f}_2 = 0.02$
$\Delta P_{TL} = 0.02$	$\Delta \hat{P}_{TL} = 0.01$

IV. Simulation Results

In this section, the dynamic stability and time response of the three different controllers are examined. We begin by examining the conventional PI controller, then we examine the observer-based servo controllers using both pole placement and LQG techniques. These responses include how frequency bias settings and inadvertent tie-line interchange flows influence the AGC response. To demonstrate the usefulness of the proposed LQG controller, computer simulations are performed using the MATLAB/SIMULINK environment for the two-area interconnected AC electrical system described in section II.

For each controller, the control inputs and state trajectories are plotted in response to nonzero initial conditions and a harsh step disturbance representing a load change of $\Delta P_D = 0.5$ p.u. in area 1. In addition, a step change of $\Delta P_{TL} = 0.1$ p.u. in the tie-line flow is scheduled. Such magnitude changes are used to examine the robustness of the controllers designed for extreme operating points and rapidly varying system conditions. The nonzero initial conditions for the state variables and state estimators are shown in Table II.

With a step disturbance in area 1 of $\Delta P_D = 0.5$ p.u., and tie-line interchange of $\Delta P_{TL} = 0.1$ p.u. the system is expected to behave as follows:

- At steady state, generation in area 1 should change by $\Delta P_C = 0.6$ p.u. to absorb its own load and interchange $\Delta P_{TL} = 0.1$ p.u., and generation in area 2 should decrease by $\Delta P_C = -0.1$ p.u.
- State trajectories for frequency deviations in both areas should be minimized and eventually eliminated.
- State trajectories for the valve position and power generation in both areas should follow the corresponding control input, i.e., 0.6 p.u. for area 1 and -0.1 p.u. in area 2.

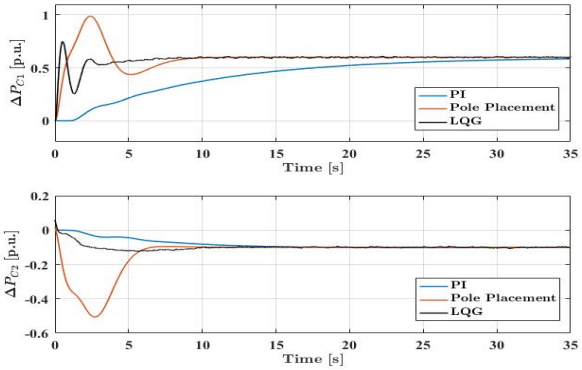

Fig. 5: Control input trajectories.

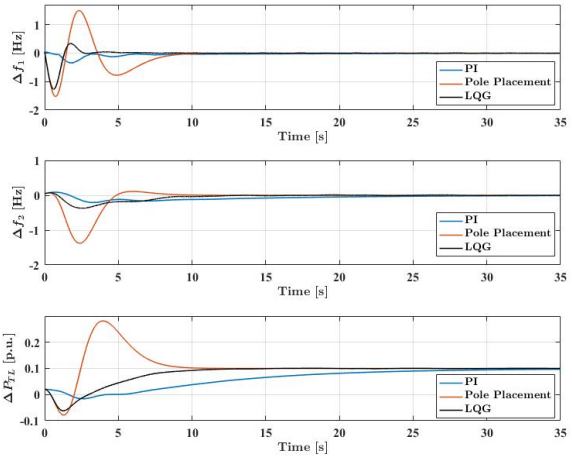

Fig. 6: Frequency and tie-line deviation state trajectories.

The time-domain responses for the three controllers are illustrated in Figs. 5–7. The classical PI controller time response is the slowest, converging in nearly 35 s. The observer-based servo controller designed through the pole placement technique shows a much improved response in terms of convergence time, about 7 s. The LQG controller further improves the response compared with the pole placement technique. The time response convergence time is improved to be 5 s. Additionally, the control input in area 2 is minimized further since the load change occurred in area 1.

V. Concluding Remarks

Sudden load changes in any interconnected multi-area power system cause frequency and tie-line interchange power deviations. It is essential to minimize these deviations for economic and reliable operation of the power system. In this paper, a comparison between the dynamic stability and time responses of three different controllers is presented for the two-area interconnected system. The conventional PI controller requires the longest time for stabilization. By comparison, the pole placement- and LQG-based controllers both achieved far less convergence time than the conventional PI controller for a sudden load step disturbance followed by a tie-line

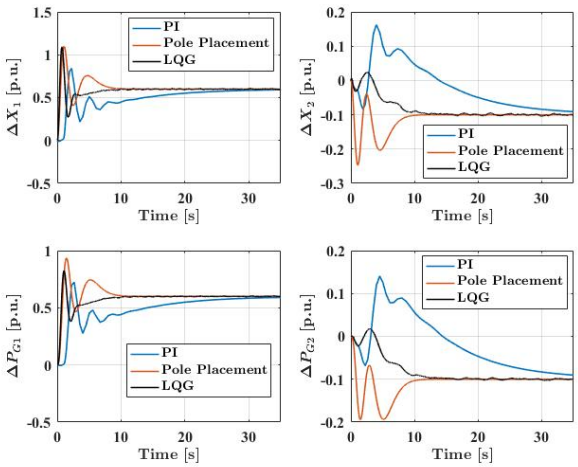

Fig. 7: Valve position state trajectories.

scheduling adjustment. Moreover, the LQG controller time response was better overall considering the influence on the second area and required control input magnitude. The main advantages of the LQG controller are intuitive tuning of design parameters, optimal trajectories regardless of disturbance size or initial conditions, and robustness against disturbance and measurement noises. Furthermore, the DT LQG controller is more practical than its CT counterpart and is preferred in view of the discrete nature of power system data.

References

[1] E. Vaahedi, *Practical Power System Operation*. Wiley-IEEE Press, 2014.

[2] N. E. Y. Kouba, M. Menaa, M. Hasni, and M. Boudour, "Load frequency control in multi-area power system based on fuzzy logic-pid controller," in *Smart Energy Grid Engineering (SEGE), 2015 IEEE International Conference on*, Aug 2015, pp. 1–6.

[3] M. R. I. Sheikh, S. M. Muyeen, R. Takahashi, T. Murata, and J. Tamura, "Application of self-tuning fpic to agc for load frequency control in multi-area power system," in *PowerTech, 2009 IEEE Bucharest*, Jun 2009, pp. 1–7.

[4] A. Morinec and F. Villaseca, "Continuous-mode automatic generation control of a three-area power system," in *The 33rd North American Control Symposium*, 2001, pp. 63–70.

[5] G. A. Chown and R. C. Hartman, "Design and experience with a fuzzy logic controller for automatic generation control (agc)," in *Power Industry Computer Applications., 1997. 20th International Conference on*, May 1997, pp. 352–357.

[6] D. Rerkpreedapong, A. Hasanović, and A. Feliachi, "Robust load frequency control using genetic algorithms and linear matrix inequalities," *IEEE Transactions on Power Systems*, vol. 18, no. 2, pp. 855–861, 2003.

[7] Y. Zhang, L. Dong, and Z. Gao, "Load frequency control for multiple-area power systems," in *American Control Conference, 2009. ACC'09.* IEEE, 2009, pp. 2773–2778.

[8] A. Aziz, A. Mto, and A. Stojsevski, "Automatic generation control of multigeneration power system," *Journal of Power and Energy Engineering*, vol. 2, no. 04, p. 312, 2014.

[9] S. Sivanagaraju, *Power system operation and control*. Pearson Education India, 2009.

[10] A. J. Wood and B. F. Wollenberg, *Power generation, operation, and control*. John Wiley & Sons, 2012.

[11] US DOE & FERC. (2006, Feb) Steps to establish a real-time transmission monitoring system for transmission owners and operators within the eastern and western interconnections. [Online]. Available: http://energy.gov/sites/prod/files/oeprod/DocumentsandMedia/final_1839.pdf